

2D PARTICLE MECHANICS SIMULATIONS ON EVOLUTION AND INTERACTIONS OF HEAT CHAINS AND FORCE NETWORKS UNDER STEADY-STATE CONDITIONS

Gülşad Küçük,^{1,*} Marcial Gonzalez,² & Alberto M. Cuitiño³

¹Department of Mechanical and Aerospace Engineering, Rutgers University, Piscataway, New Jersey, 08854, USA

²School of Mechanical Engineering Purdue University 585 Purdue Mall West Lafayette, Indiana 47907-2088, USA

³Department of Mechanical and Aerospace Engineering, Rutgers University, Piscataway, New Jersey, 08854, USA

*Address all correspondence to: Gülşad Küçük, E-mail: gulsad@gmail.com

Unlike continuum media, granular materials host an inhomogeneous distribution of contact networks, which results in an uneven distribution of loads inside the dense particulate assemblies. These structural arrangements play a critical role in determining the preferred paths of heat transport, due to the fact that thermal contact conductance is a function of the contact interfaces formed between particles. In spite of recent experimental and theoretical studies on the evolution of force chains, the formation of heat chains and the correlation between them still remain unclear. In this regard, a two-dimensional discrete model based on a particle mechanics approach is developed to unveil the characteristics of these microstructural arrangements, and the interactions between them under steady-state and equilibrium conditions. Thermally-assisted compaction of powders is a widely used manufacturing technique. Therefore, in this work, we model a two-dimensional configuration of randomly distributed spherical particles confined in a rigid die under mechanical and thermal loads. For this particular configuration, we study fundamental concepts such as formation of force and heat chains, evolution of force and heat distributions with respect to compaction parameters, and cross-property relation between normal force and heat transferred at the contact surfaces.

KEY WORDS: *thermomechanical coupling, heat networks, force networks, cross-property relation, granular materials, contact mechanics*

1. INTRODUCTION

Designing materials based on the required properties of the end product, such as mechanical strength, and thermal and electrical conductivity, is contingent upon the knowledge of the interparticle relations that determine the microstructure of the confined particulate system. In recognition of the unique characteristics of granular materials, the multiphysics behind the thermomechanically coupled deformation plays a critical role in formation of structural arrangements that reveal highly inhomoge-

neous paths of heat and force transfer within the granular assembly. Understanding the evolution and interactions of these pathways, particularly in response to boundary conditions and system parameters, represents a fundamental goal of granular mechanics, in terms of estimating and optimizing their collective behavior on macroscopic material properties.

Experimental studies on static and dynamic granular systems reveal a highly heterogeneous distribution of force network formation, which is impossible to observe in a solid, liquid, or gas (Jaeger et al., 1996). Visualization

of interparticle forces in a granular media by photoelastic or carbon paper techniques shows that special structural arrangements arose to serve the purpose of supporting most of the external load, while leaving the other particles unloaded or less loaded (Blair et al., 2001; Løvoll et al., 1999; Majmudar and Behringer, 2005; Mueth et al., 1998; Snoeijer et al., 2004). The force chains can be treated as the load bridges, which usually stand several times larger forces than the rest of the system (Antony, 2007). In static silos these mechanisms are responsible for enhancing arch formations and in dynamic loading cases altering deformation patterns. It has been also argued that uneven distribution of force chains causes localized fracture and hot spot formations where the process may trigger chemical wave front propagation or phase transition, due to the instant change of temperature or redundant contact forces (Roessig et al., 2002).

More recently, a study on packing grains by thermal cycling elucidated the collective behavior of particulate materials and became an inspiration for various engineering applications. Chen and co-workers investigated the influence of thermal cycling on packing fraction by examining a loosely packed bed of glass beads in a plastic container (Chen et al., 2006). The difference in thermal expansion property of the beads and the container is shown to have a critical effect on beads rearrangement, which is similar to mechanical agitation on altering grain packing (Chen et al., 2006). It is also proved that arch formations within the granular assemblies lead up to giant stress fluctuations that are mostly associated with the extreme sensitivity of stress paths to small perturbations, such as applied thermal gradient on the granular system (Claudin and Bouchaud, 1997; Liu and Nagel, 1992).

Due to the fact that traditional material examination methods, which mostly rely on postprocess characterization, provide very poor or inaccurate information. In the prospect of revealing the driving mechanisms, there exists an inevitable need for simulations based on detailed microlevel information. In this regard two major approaches have been adopted to unveil the formation of force distributions within granular assemblies. These approaches differ by how they define the initial problem, which consists of a continuum media and a discrete system of particles. The well-known paper in the former group is a stochastic model, named as “q-model,” that explains the probability distribution of contact forces in bead packs by using statistical mechanics (Liu et al., 1995). Also being proved by experimental studies, this model suggests that normal contact force distribution obeys a decaying exponential law for the forces that are above the average (Claudin

and Bouchaud, 1997; Coppersmith et al., 1996; Liu et al., 1995). The latter approach works on particle interactions and the constitutive relations of contact mechanics. Discrete element methodology has been widely used in the field of particle scale research (Zhu et al., 2007). The early work of Cundall and Strack on granular dynamics is based on an explicit numerical scheme, through which the particles; interactions are calculated over the contact networks and particle motion is determined by the state of force balance equilibrium (Cundall and Strack, 1979). This technique is adopted by many engineering fields to analyze the dynamic, quasi-static and static stress-strain behavior of an assembly of distinct objects (Makse et al., 2000; Radjai et al., 1996; Radjai and Roux, 1995).

The problem of thermally-assisted compaction entails the integration of contact mechanics principles with thermal-contact model analytical solutions to account for the effective modeling of heat conduction within the deformed state of granular materials. In this regard Vargas and McCarthy introduced a thermal particle dynamics model, by which they track the formation of stress and heat front evolution during heat conduction through a packed bed of cylinders (Vargas and McCarthy, 2001). They showed that similar to stress chains, there exist preferable paths to conduct heat within the granular bed, which are recalled as heat chains. Surprisingly, stress chains and heat chains are not identical; however, they share the same characteristic of being unevenly distributed and being dependent on the loading conditions (Vargas and McCarthy, 2001, 2007). Feng et al. extended the numerical methodology used in discrete element modeling for systems comprising a large number of circular particles in 2D cases (Feng et al., 2008). Starting from the analytical integral solution for the temperature distribution over a circular body, a system of thermal conductivity equations is derived in terms of the average temperatures and the resultant fluxes at the contact zones with the neighboring particles (Feng et al., 2008). Unlike the finite element method, discrete mechanics provide a very reasonable solution accuracy, where it has also no discretization errors involved in the numerical assessments (Feng et al., 2008). Even though there still exist computational challenges in carrying out calculations on a large number of particles, which undergo highly nonlinear system of coupled deformations, in this research we work on advances in numerical methods to enhance the feasibility and efficiency of computational mechanics.

It is the purpose of this study to provide that insight into the nature of thermomechanical interactions, that determine the microstructure formation of the thermally-

assisted compaction of granular assemblies. We consider a packed two-dimensional arrangement of spherical particles compressed by heated boundary walls. We introduce a particle mechanics approach to simulate multibody system characteristics of granular beds starting from the pair interactions of particles defined by thermoelastic contact models. We trace the evolution of contact networks under steady state conditions and address the intriguing question of how the force networks are related to heat chains. Finally we compare the effects of four different boundary conditions on the formation of these structural elements.

2. PARTICLE MECHANICS APPROACH

We present a multi-body framework starting from the pair interactions of particles defined by thermoelastic contact models. This concept is similar to recent studies of Vargas and McCarthy (2001), and Vargas and McCarthy (2007), where they introduce a mathematical model as an extension to the discrete element model of granular materials. However, our approach is based on defining particles' final state, such as position and temperature, rather than tracing particles during the compaction process. Details of the approach adopted in this study can also be found in our earlier work (Küçük et al., 2016).

Our point of departure for the discrete model is to integrate the well-known theory of Hertzian deformation for quasi-static mechanics and conductive heat transfer for spherical conforming contacts of granular media. The temperature and the position of particles are obtained through the equilibrium for the system particles. The total heat transferred to individual particle m from neighboring particles n and the total of forces acting on particle m are equated to zero.

$$Q^m = \sum_{n \in \mathcal{N}_m} Q^{mn} = 0, \quad (1)$$

$$\mathbf{F}^m = \sum_{n \in \mathcal{N}_m} F^{mn} \mathbf{n}^{mn} = 0, \quad (2)$$

where \mathbf{n}^{mn} is the unit normal vector defined from centers of particle n to particle m .

$$\mathbf{n}^{mn} = \frac{\mathbf{x}^m - \mathbf{x}^n}{\|\mathbf{x}^m - \mathbf{x}^n\|}. \quad (3)$$

Johnson states the well-rounded contact mechanics considerations that explain the elastic deformation of locally spherical particles under compression loads in his

book (Johnson, 1987). It is also assumed in this study that small-strain deformation of conforming surfaces results in a flat circle of contact area. Collinear contact force at this elastic contact of the particles m and n is defined through Young's moduli, E^m and E^n ; Poisson's ratios, ν^m and ν^n ; particle radii, R^m and R^n ; and overlap, γ^{mn} , between these particles.

$$F^{mn} = \frac{4}{3} E^{mn} (R^{mn})^{1/2} (\gamma^{mn})^{3/2}, \quad (4)$$

where

$$R^{mn} = \left[\frac{1}{R^m} + \frac{1}{R^n} \right]^{-1}, \quad (5)$$

$$E^{mn} = \left[\frac{1 - (\nu^m)^2}{E_m} + \frac{1 - (\nu^n)^2}{E_n} \right]^{-1}, \quad (6)$$

$$\gamma^{mn} = R^m + R^n - \|\mathbf{x}^m - \mathbf{x}^n\| \quad (7)$$

Vargas and McCarthy (2007) One particular effect of applied thermal load on the system of particles is the change in radii due to thermal expansion. Similar to previous studies in the literature Lu et al. (2001); Vargas and McCarthy (2007), in the present study, linear thermal expansion formulation is taken into consideration.

$$R^m = R_{ref}^m [1 + \alpha^m (T^m - T_{ref}^m)], \quad (8)$$

where α^m is the thermal expansion coefficient, T_{ref} is the reference temperature, and R_{ref}^m is the radius of particle at the reference temperature. Due to the dependence of contact geometry on the nature of a thermomechanically coupled problem, it is expected to capture a distribution of contact area formation throughout the compacted medium.

There has been considerable research on modeling the thermal contact of deformed bodies. The major heat transfer mechanisms are conduction through solid, conduction through the contact area between two touching particles, conduction to/from interstitial fluid, heat transfer via convection, and radiation between particle surfaces, radiation between neighboring voids (Vargas and McCarthy, 2001). Under the prescribed thermally-assisted compaction conditions in this study, the first two of the above are assumed to be the main contributors in heat transfer through the particulate bed. The problem of heat transfer regarding the compaction of particles, which are in or nearly in contact, is deeply investigated by a number researchers (Batchelor and O'Brien, 1977; Chan and Tien, 1973; Kaganer, 1966). In this study we adopt Batchelor and O'Brien's thermal-contact model. In an attempt

to find the approximate effective thermal conductivity of ordered and randomly packed granular beds, Batchelor and O'Brien calculated the heat flux across the flat circle of contact between smooth, conforming, and elastic particles.

$$Q^{mn} = H^{mn}(T^m - T^n), \quad (9)$$

$$H^{mn} = 2a^{mn}k^{mn}. \quad (10)$$

H^{mn} is contact conductance, which defines the ability of two conforming particles to transmit heat across their mutual interface. k^{mn} is the arithmetic mean of the thermal conductivities of two particles in contact, and a^{mn} is the Hertzian contact area.

$$k^{mn} = \frac{1}{2} \left[\frac{1}{k^m} + \frac{1}{k^n} \right]^{-1}, \quad (11)$$

$$a^{mn} = \sqrt{\gamma^{mn} R^{mn}}. \quad (12)$$

The total heat flow to an individual particle, [Eq. (1)], is calculated by adding the heat flow at each contact of the particle between its neighboring particles [Eq. (9)]. In the current study, we assume that the temperature at each contact of an individual particle is equal to the temperature calculated at the center of the particle. In other words the temperature does not vary significantly within the particle, which also imposes that the contact conductance along the mutual interface of conforming particles is relatively smaller than the heat conductance within the particle.

$$\frac{2k^{mn}a^{mn}}{k^{mn}A/R^m} \ll 1 \quad (13)$$

where A is the cross-sectional area, $\pi(R^m)^2$. In other words the expression given in Eq. (13) defines the state of Biot number much less than 1. This assertion is applied by several authors in earlier studies (Siu and Lee, 2004; Vargas and McCarthy, 2001). The condition of $a^{mn} \ll R^{mn}$ is also required by the small-strain contact mechanics model.

2.1 Methodology

Random packing of particles is generated by using the ballistic deposition technique, which was developed by Gioia et al. (2002). Based on the gradually applied thermal and mechanical boundary conditions, interparticle and wall-particle interactions are estimated. Starting from an initial guess for the position and temperature of the particles, a system of nonlinear equations that define the

force and heat transfer at each particle are solved at quasi-static mechanical and steady-state thermal equilibrium. The Newton-Raphson method is implemented in the direct iterative solution. Rigid wall assumptions are used in evaluating the state of boundary particles, which are in contact with walls. Analogous to the ghost-cell method, boundary particle-adjacent wall interaction is simulated as the contact between a particle and a ghost particle, where both are symmetrically deformed. The ghost particle is assumed to have the same material properties and radius as the boundary particle. The boundary wall is assumed to be located in the midst of these symmetrically deformed particles. The temperature difference between the ghost particle and the wall surface is the same as the temperature difference between the wall surface and the boundary particle.

2.2 Simulation Configuration

In the two-dimensional numerical experiments the particles are shown as circles, and the boundary walls are presented with solid lines. Initially the particles are assumed to be at point contact; upon the application of thermal and mechanical loads the particles change place and settle down while reaching a steady-state temperature to adjust with the overall temperature gradient of the system. Incremental deformations are applied in a quasi-static manner, beginning with a stress-free state. In order to avoid the dominant influence of boundaries and to minimize the local fluctuations of spatially dependent properties, we focus on a particulate system, which is a few tens of particles diameter. This concept has been confirmed to provide statistical homogeneity by Radjai et al. (1996) and verified by previous experimental studies of Emeriault and Cambou (1996); Rothenburg and Bathurst (1989).

As shown in Fig. 1 initial configuration is a randomly arranged bed of 2077 stainless steel particles with Young's modulus, E , 193 GPa; thermal conductivity, k , 15 W/m K; Poisson's ratio, ν , 0.29; thermal expansion, α , 17.3×10^{-6} 1/K. The particles of 4 mm in radius are contained in a bed of 0.4 m in width and height, L . Compression along the yy direction is created by the incremental downward movement of the top wall, which acts a punch. The other three walls are fixed and kept at reference temperature. The total strain, $\epsilon_{yy} = |\Delta L/L|$, applied on the system is equal to the compaction ratio. In order to consider the effect of temperature increase and thermal expansion, a thermal gradient is induced through the top heated wall and the particles in touch with this boundary. The packing density of the undeformed system of parti-

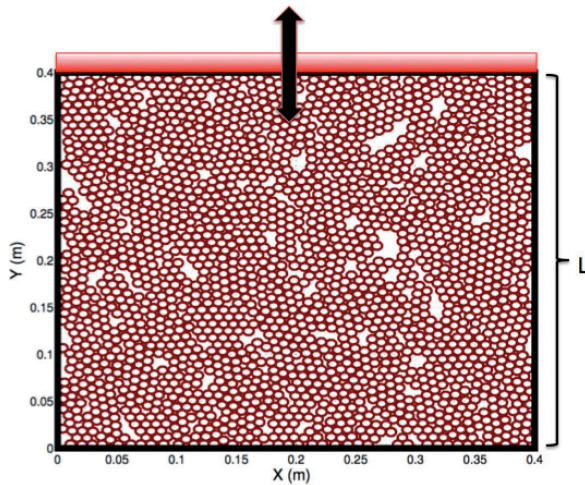


FIG. 1: Undeformed configuration of a 2077-particle system. Initial length in the x and y direction is 0.4 m.

cles is 0.72. The weight of the particles is neglected in two-dimensional analysis.

3. FUNDAMENTAL CONCEPTS IN 2D PARTICLE MECHANICS MODELING OF GRANULAR MATERIALS

Based on the proposed particle mechanics approach, we conduct a numerical analysis to exploit the dependence of the contact network with regard to the formation of force and heat chains within the confined granular bed. We investigate the normal contact force and heat distributions in the prospect of understanding the cross-property connection between force and heat distributions.

3.1 Formation of Force Networks

Force chains that form the skeleton of compacted granular materials (Ostojic et al., 2006), can be visualized by representing normal forces at contacts as bonds between the conforming particles. The thickness of the line segment connecting the particles is proportional to the magnitude of the normal contact force that is above the average. In force and heat chain representations, we plot the particles as circles filled with black color, and surrounded by a red line. The force chains are shown as blue lines. To provide a more traceable visualization we prefer to show the heat gradient within the particulate bed, by altering the color filling of each particle. In the following figures the fill-

ing color of circles is changed from black to red, as the temperature of particles increases.

For a system of 2077 stainless steel particles, initially we consider two cases of compaction. In both cases mechanical deformation is imposed gradually by moving the top wall. The total deformation is $\epsilon_{yy} = 0.08$. In the first case the boundary walls are kept at a reference temperature of 293 K, whereas in the second case only the top wall is elevated to a higher temperature of 493 K while keeping the other three walls at 293 K. The formation of force chains in the former case, which is a purely mechanical deformation, is plotted in Fig. 2(a).

In Fig. 2(b) the thickness of the line segments is seen to be relatively decreased, and the intensity of horizontal force chains is increased. It is also observed that thermal gradient is inducing larger contact forces around the heated punch.

3.2 Contact Force Distribution

A widely used characterization parameter to quantify the formation of force chains is the probability distribution of individual contact forces. There exists a broad spectrum of statistical mechanics studies (Coppersmith et al., 1996; Liu et al., 1995; Makse et al., 2000; Snoeijer et al., 2004) and experimental studies (Blair et al., 2001; Løvøll et al., 1999; Majmudar and Behringer, 2005; Roessig et al., 2002) developed to estimate the probability of normal contact force distribution within static and consolidated granular materials. The force distributions are expressed in terms of a nondimensional variable, f , that defines the normal force at the contact divided by the average of these contact forces, $f = F/F_{ave}$. In a typical granular packing, the probability distribution, $P(f)$, has an exponentially decaying tail at $f > 1$, and a plateau at $f < 1$.

Based on our particle mechanics approach we trace the normal contact forces that are above the average, at each contact. In Fig. 3 we plot the distribution of normalized contact forces f for the system of 2077 particles that is compressed by the downward movement of the top boundary. The total strain, $\epsilon_{yy} = \Delta L/L$, imposed on the system is 0.08, and no thermal gradient is applied. We estimate the normalized contact force distribution by an exponential decay function, which can be shown as

$$D(f) \propto e^{\beta f}, \quad f > 1, \quad (14)$$

where $\beta = -1.4722$.

We investigate the dependence of packing fraction on the contact force distribution. The system of 2077

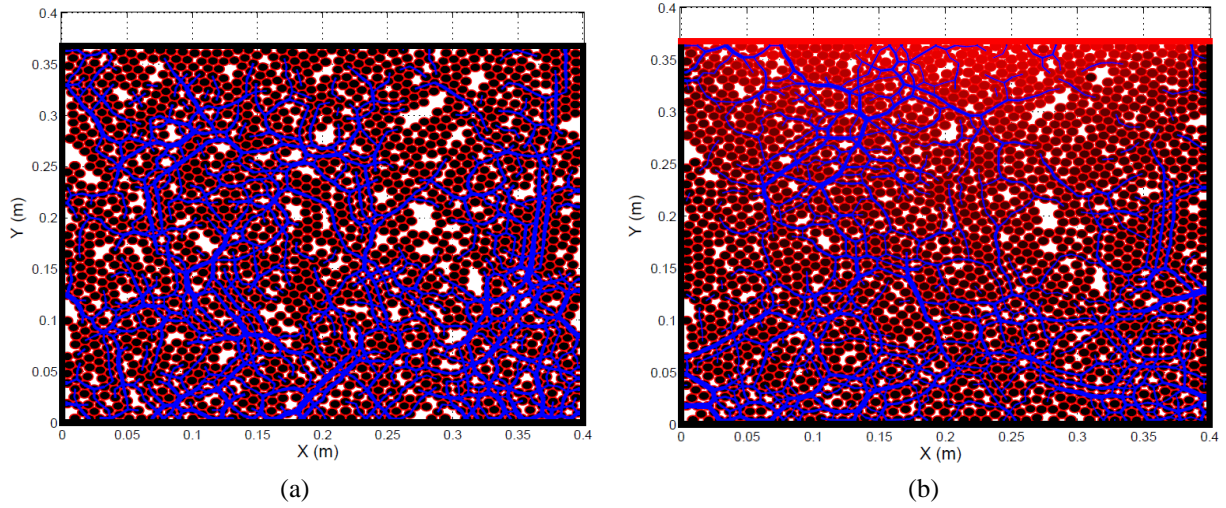


FIG. 2: Force chains developed in compaction of 2077 stainless steel particles system. Compaction strain, $\epsilon_{yy} = |\Delta L/L| = 0.08$. **(a)** Particle system under the sole effect of mechanical deformation, **(b)** Particle system under the coupled field of thermal and mechanical deformation. $T_{punch} = 493$ K

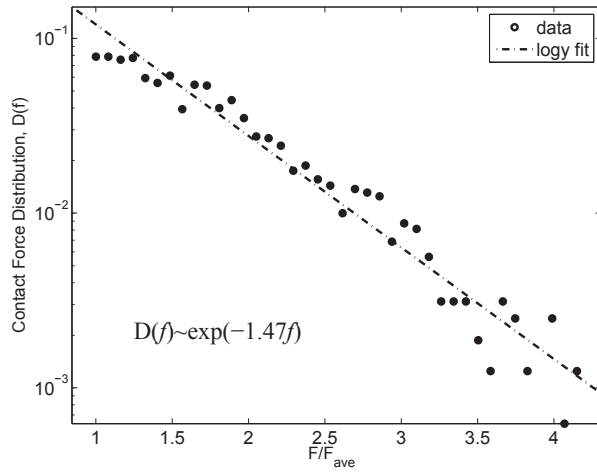


FIG. 3: Normalized contact force distribution of athermally compacted system of 2077 stainless steel SS304, particles

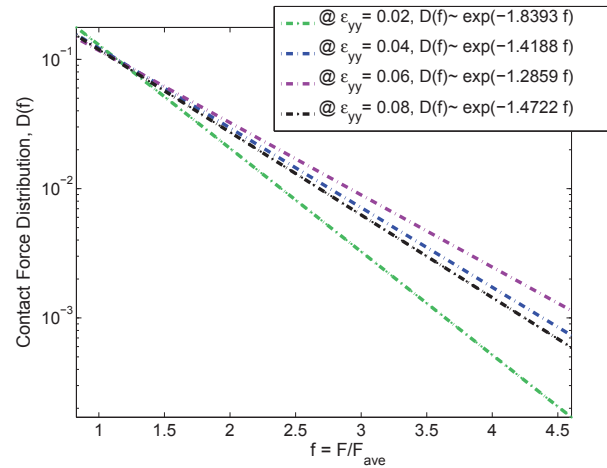


FIG. 4: Comparison of force distributions for a gradually compacted system of 2077 particles. The total strain is $\epsilon_{yy} = |\Delta L/L| = 0.08$.

particles is gradually compressed by lowering the top wall. The normalized force distributions of the contacts are evaluated at compaction rates, 2%, 4%, 6%, and 8%.

In the absence of applied thermal gradient on the system, the normalized contact force distributions coincide over at the range of $\beta \approx -1.4 \pm 0.1$, as seen in Fig. 4.

The off-range value obtained at $\epsilon_{yy} = 0.02$ is attributed to the loosely packed structure of the contact network. In Fig. 5 the normalized contact force distributions are plotted when the top wall, the punch, is kept at a temperature of 493 K. Although the general trend of the distribution is the same, a remarkable change in the exponential power is experienced, $\beta^T \approx -0.85 \pm 0.25$.

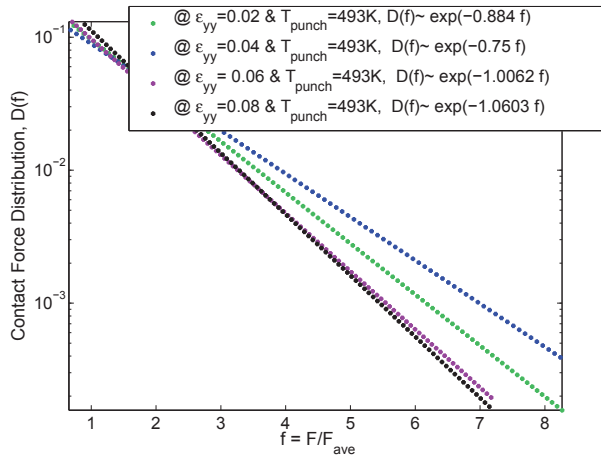


FIG. 5: Comparison of force distributions for a gradually compacted system of 2077 particles. The total strain is $\epsilon_{yy} = |\Delta L/L| = 0.08$. Punch temperature is kept at 493 K.

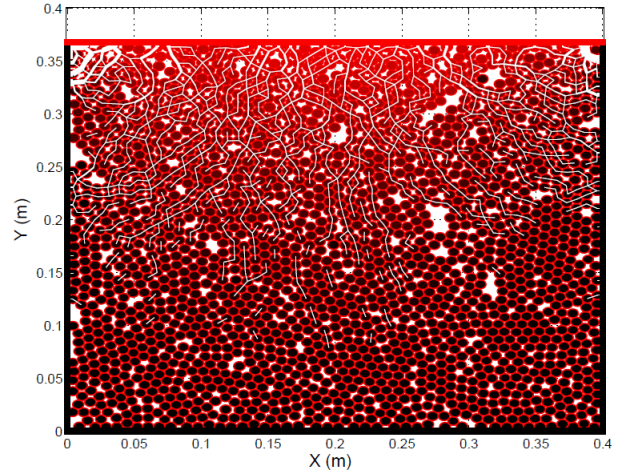


FIG. 6: Heat chains developed in thermally-assisted compaction of a system of 2077 stainless steel particles system. Punch temperature is kept at 493 K. The total mechanical deformation is $\epsilon_{yy} = |\Delta L/L| = 0.08$

3.3 Formation of Heat Chains

During the process of thermally-assisted compaction, the confined granular bed is under the effect of a thermal gradient, which triggers a formation of preferred paths of heat transport within the assembly. In order to visualize the heat chains, we use a similar approach as in the evaluation of force chains. The heat transferred at each contact is mapped into the contact network, shown in lines whose thickness is proportional to the heat flux. In Fig. 6, we represent the heat chains developed in the system of 2077 randomly packed particles that are compacted by a ratio of 8% and heated through the top wall, which is kept at 493 K.

Unlike the force network, the heat chains are accumulated closely to the boundary at the elevated temperature. Although heat conductance is a function of the contact area between the conforming surfaces, Fig. 6 shows that the preferred paths of heat transfer depend strongly on the spatial orientation of applied thermal gradient on the particulate bed.

3.4 Heat Distribution

Similar to force distribution analysis, we investigate the heat distribution within the contact network. The numerical simulations point out that the normalized heat distribution can be distinctly expressed in log-log plots. In Fig. 7 the heat distribution of the 2077-particles system is

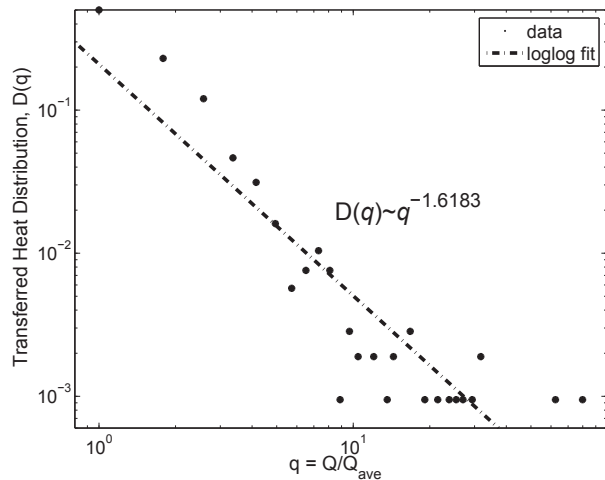


FIG. 7: Normalized heat distribution of 2077 stainless steel particles' system $T_{punch} = 493$ K and the total strain, $\epsilon_{yy} = 0.08$

shown for the particular loading of compaction ratio, $\epsilon_{yy} = 0.08$, and the top wall is kept at 493 K.

$$D(q) \propto q^\zeta, \quad Q > Q_{ave}, \quad (15)$$

where $\zeta = -1.6183$. In order to understand the effect of applied thermal gradient on the heat distribution characteristics, the same system is investigated in a gradually heated numerical experiment. The particle assembly is

compacted by a ratio of 8%, and the temperature of the top wall is increased from 293 to 493 K, by increments of 40 K. Figure 8 summarizes that $D(q) \approx q^{-1.7 \pm 0.1}$ for the particular thermal gradient range.

3.5 Cross-Property Relation between Force and Heat Distributions

In this study we aim to quantitatively explain the role of heat transfer in contact force distribution and the role of the compaction ratio in heat transfer distribution within the particulate bed. Figure 9 points out one of the unique characteristics of thermally-assisted compaction. The exponential power, which indicates distribution of contact forces above the mean, decreases up to 25% of its initial value, as the applied thermal gradient on the system is increased. Although we observe the peak around the same mean, the system, which is under a larger thermal load, has a much slower decaying exponential tail. It is a clear sign of a more uniform microstructure with less-deep fluctuations in distribution of contact forces. The applied thermal gradient not only changes the particle re-arrangement and packing density remarkably, as explained earlier in Chen et al. (2006), but also has a significant effect on the contact force distributions of the confined granular medium.

In Fig. 10 heat distributions of a gradually heated confined system of particles are traced. The correlation between heat distribution and compaction ratio reveals that the packing density plays a critical role in determining the

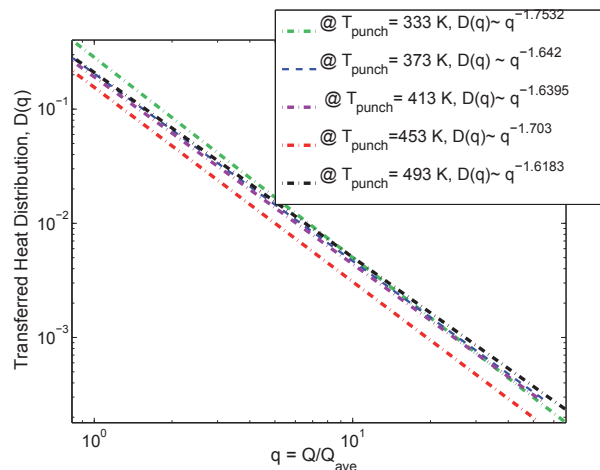


FIG. 8: Comparison of heat distributions for a gradually heated system of 2077 particles, under effect of the total thermal gradient of 200 K, and the total strain, $\epsilon_{yy} = 0.08$

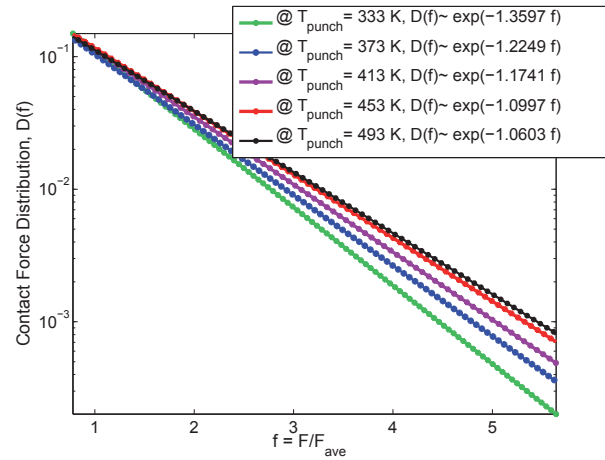


FIG. 9: Comparison of force distributions under different thermal boundary conditions. The system of 2077 stainless steel particles is compacted by a ratio of 8%, while the thermal gradient imposed between the top and bottom boundary walls is increased from 40 to 200 K, gradually

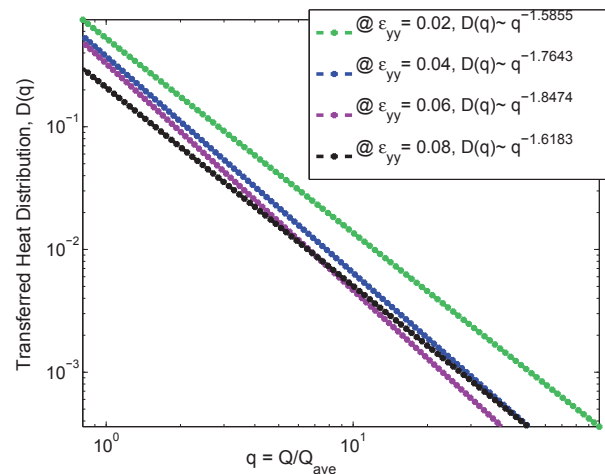


FIG. 10: Comparison of heat distributions under different mechanical loading conditions. System of 2077 stainless steel particles is under the effect of a thermal gradient, 200 K, while it is compacted up to a ratio of 8%, gradually

steady-state solution of the system. The power exponent, which characterizes the heat distribution, seems to converge at the same value $\zeta^e \approx -1.7 \pm 0.1$, over a certain packing density. Although the formation of heat chains deviates significantly from the formations of force chains, the main mechanism that determines the overall heat dis-

tribution is dominantly controlled by the contact network formation.

In the view of these findings, we would like to underline a characteristic about the current simulation configuration. Similar to previous experimental and numerical studies, the exponential distribution of contact forces accounts for 40%, and power law decay of heat distribution constitutes 30%, of all contacts. It is also important to note that the extremely large values seen as a rare sequence in normalized distributions of force and heat are due to the contacts between particles and boundary walls. Furthermore we suggest that, to obtain more accurate and predictive models at moderate levels of deformation and high confinement, the Hertz law can be replaced by the non-local contact formulation (Gonzalez and Cuitiño, 2012, 2016).

4. A CASE STUDY: EVOLUTION AND INTERACTION OF HEAT CHAINS AND FORCE NETWORKS DURING THERMALLY-ASSISTED COMPACTION OF A GRANULAR SYSTEM

Thermally-assisted compaction of granular systems can be achieved in various loading conditions. In this study, we mainly focus on the effects of imposing a thermal gradient in different directions. We consider the system of 2077 identical stainless steel particles to compare the evolution and interactions of heat chains and force networks developed under four different loading conditions. The initial system before thermally-assisted compaction is 0.4 m in height and width. Boundary condition 1 (b.c.1) is the case (as discussed in earlier sections of this study) in which the particle bed is confined by the downward movement of the top wall (punch), and this punch is kept at an elevated temperature. In boundary condition 2, the thermal gradient is applied though heating the side walls, and the punch and bottom wall are kept at reference temperature. Boundary condition 3 is similar to boundary condition 1, except this time the bottom wall is also kept at elevated temperature. Finally we consider a case, that is also called isotropic compaction in the literature. For a 2D simulation of this setup, we keep the top wall and right-hand side wall at elevated temperature. In this boundary condition (b.c.4), the heated walls are also acting as punches; in other words, the top wall is moving down, and the right wall is moving to the left to compress the system of particles. We consider the case when the heated walls' temperature is set to be 393 K, and total compaction strain is 8%. For the case of isotropic compression $\epsilon_{xx} = \epsilon_{yy} = 0.04$. The force networks developed

under the boundary conditions 1, 2, 3, and 4 are shown in Figs. 11, 12, 13, and 14, respectively.

In Fig. 15 we compare the contact force distributions generated inside a confined granular bed under the four different boundary conditions. Having the fastest decay in the exponential tail, boundary condition 4 reveals the most uniform contact force distribution. The similarity in profiles observed in boundary conditions 1 and 3, and the difference in boundary condition 2, suggest that the di-

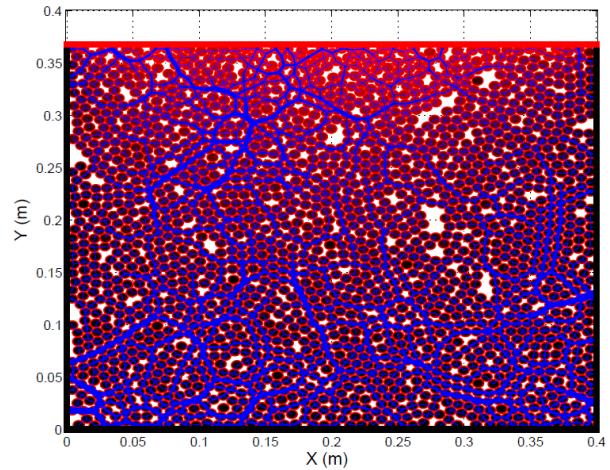


FIG. 11: Force networks developed under boundary condition 1, $\epsilon_{yy} = |\Delta L/L| = 0.08$, $\epsilon_{xx} = 0$, $T_{TopWall} = T_{punch} = 393$ K, $T_{SideWalls} = T_{BottomWall} = 293$ K

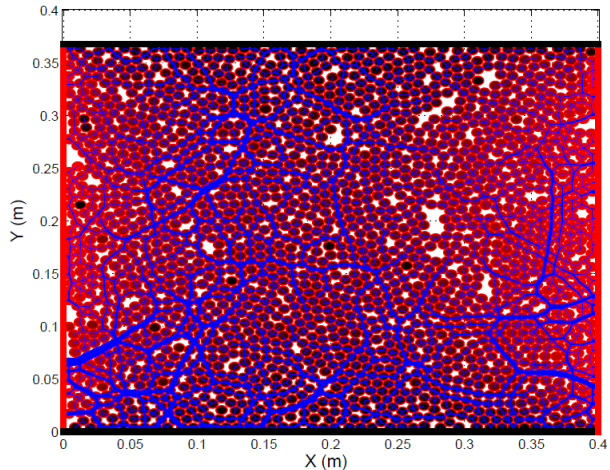


FIG. 12: Force networks developed under boundary condition 2, $\epsilon_{yy} = |\Delta L/L| = 0.08$, $\epsilon_{xx} = 0$, $T_{SideWalls} = 393$ K, $T_{punch} = T_{ref} = 293$ K

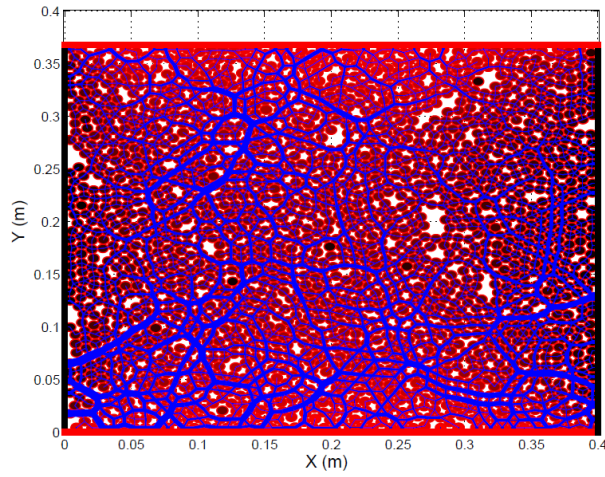


FIG. 13: Force networks developed under boundary condition 3, $\epsilon_{yy} = |\Delta L/L| = 0.08$, $\epsilon_{xx} = 0$, $T_{TopWall} = T_{punch} = 393$ K, $T_{BottomWall} = 293$ K, $T_{SideWalls} = 293$ K

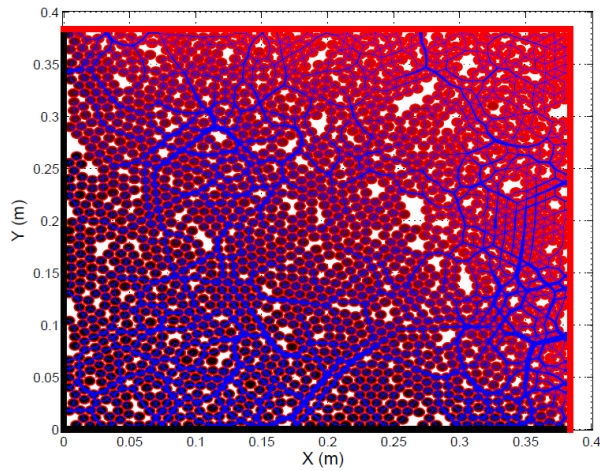


FIG. 14: Force networks developed under boundary condition 4, $\epsilon_{yy} = |\Delta L/L| = 0.04$, $\epsilon_{xx} = 0$, $T_{TopWall} = T_{punch} = 393$ K, $T_{BottomWall} = 293$ K, $T_{SideWalls} = 293$ K

rection of imposed thermal and mechanical loads significantly affects the evolution of force networks. We also claim that in the case of boundary condition 2, thermal expansion due to a transversely applied thermal gradient and the mechanical strain under the effect of macroscopic compaction force enhance the nonuniformity of force distribution and increase the probability of observing

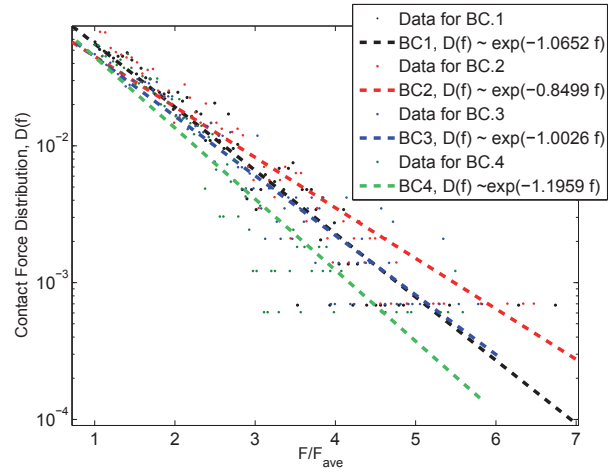


FIG. 15: Comparison of normalized contact force distributions for different boundary conditions

larger values of contact forces at particular pair interactions.

Regarding the system of 2077 stainless steel spherical particles, which is compacted by a compaction strain of 8% of its initial height and is under an imposed thermal gradient of 100 K, Fig. 16 shows that heat network generation and heat distribution at the contacts do not vary significantly under these boundary conditions.

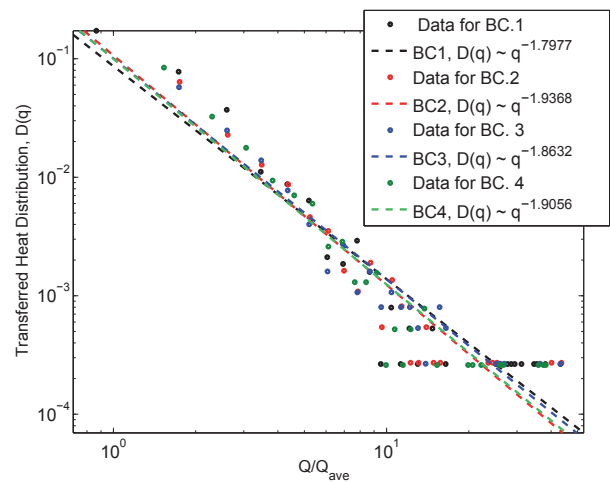


FIG. 16: Comparison of heat distributions for different boundary conditions

5. CONCLUSIONS

Particle scale modeling of thermally-assisted compaction requires the extension of the discrete element method to account for the effective modeling of heat conduction, which indeed is similar in spirit to understanding and developing platforms for other widely encountered coupled phenomena such as thermoelectrical and electromechanical processes. The two important contributions of the present work to coupled problems in general, and to thermomechanical problems in particular, are (i) the development of a particle mechanics approach that unveils key characteristics of thermally-assisted compaction of large, two-dimensional systems comprised of spherical particles; (ii) a numerical methodology for unveiling the cross-property connection between the probability distributions of force and heat networks, which determine the macroscopic properties of the consolidated material.

Our numerical methodology is capable of capturing the network of contact forces and heat fluxes within the granular bed. Despite the fact that these chains visually reveal localization of hot zones and potential arching spots, it is not feasible to trace their formation and breakage within the microstructure for large granular systems. However, the probability distributions of forces and heat fluxes provide significant insight to understand the driving mechanisms in a statistical manner.

Simulations show that the probability distribution of contact forces in a densely packed system of spherical particles is peaked about an average contact force, which is determined by the loading conditions and the material properties of the particles. For values larger than the average contact force, this distribution tends to decay out obeying an exponential power law. The observation of extremely large values of contact forces suggests that the analysis of microcrack formation is a potential area of future research. In contrast, the investigation of the probability distribution of heat fluxes indicates this distribution obeys a general decaying power law.

The complex phenomena observed in particulate systems during thermally-assisted compaction call for the need of numerical simulations that enable the determination of the relationship between probability distributions of force and heat networks as a function of the thermal gradient and the compaction ratio used in the process. Our numerical results show that the thermomechanical coupling enhances the uneven distributions of force chains. Specifically, thermally-assisted compaction not only induces larger contact forces but it also increases the frequency of observing forces larger than the average. In ad-

dition, the correlation between the probability distribution of heat fluxes and the compaction ratio reveals that the force network becomes the dominant mechanism in determining the heat network. This is more evident at high levels of compaction. It is worth noting that the threshold at which the distribution of stresses becomes the controlling mechanism is contingent upon the thermal transport properties of the consolidated system of particles.

In an attempt to use the proposed mathematical framework to predict the overall characteristics of force network generation within the thermally-assisted compacted system of particles, four typical loading conditions that mainly differ by the direction of imposed thermal gradient are considered. From a particle-level consideration of conditions required to compact a densely packed granular bed, two major conclusions that would appear to be strongly supported by experimental studies in the literature are revealed; (i) Isotropic compaction provides the most uniform contact force network formation in thermally-assisted manufacturing processes. (ii) If the thermal and mechanical deformations are applied in the transverse direction, the competing strains due to these two mechanisms increase the probability and frequency of observing extremely large values of contact forces. This effect is presumably lessened for an aligned arrangement of the applied thermal and mechanical loading conditions.

ACKNOWLEDGMENTS

This work has been partially supported by U.S. Army ARDEC grant under the project titled as: Multifunctional Nanomaterials: Processing, Properties, and Applications. The authors would also like to acknowledge the support provided by the National Science Foundation Engineering Research Center for Structured Organic Particle Systems (C-SOPS).

REFERENCES

- Antony, S., Link between single-particle properties and macroscopic properties in particulate assemblies: role of structures within structures, *Philos. Trans. R. Soc. A*, vol. **365**, no. 1861, pp. 2879–2891, 2007.
- Batchelor, G. and O'Brien, R., Thermal or electrical conduction through a granular material, *Proc. R. Soc. London, Ser. A*, vol. **355**, no. 1682, pp. 313–333, 1977.
- Blair, D. L., Mueggenburg, N. W., Marshall, A. H., Jaeger, H. M., and Nagel, S. R., Force distributions in three-dimensional granular assemblies: Effects of packing order

- and interparticle friction, *Phys. Rev. E*, vol. **63**, no. 4, p. 041304, 2001.
- Chan, C. and Tien, C., Conductance of packed spheres in vacuum, *J. Heat Transfer*, vol. **95**, no. 3, pp. 302–308, 1973.
- Chen, K., Cole, J., Conger, C., Draskovic, J., Lohr, M., Klein, K., Scheidemantel, T., and Schiffer, P., Granular materials: Packing grains by thermal cycling, *Nature*, vol. **442**, no. 7100, p. 257, 2006.
- Claudin, P. and Bouchaud, J.-P., Static avalanches and giant stress fluctuations in silos, *Phys. Rev. Lett.*, vol. **78**, no. 2, p. 231, 1997.
- Coppersmith, S., Liu, C.-H., Majumdar, S., Narayan, O., and Witten, T., Model for force fluctuations in bead packs, *Phys. Rev. E*, vol. **53**, no. 5, p. 4673, 1996.
- Cundall, P. A. and Strack, O. D., A discrete numerical model for granular assemblies, *Geotechnique*, vol. **29**, no. 1, pp. 47–65, 1979.
- Emeriault, F. and Cambou, B., Micromechanical modelling of anisotropic non-linear elasticity of granular medium, *Int. J. Solids Struct.*, vol. **33**, no. 18, pp. 2591–2607, 1996.
- Feng, Y., Han, K., Li, C., and Owen, D., Discrete thermal element modelling of heat conduction in particle systems: Basic formulations, *J. Comput. Phys.*, vol. **227**, no. 10, pp. 5072–5089, 2008.
- Gioia, G., Cuitiño, A. M., Zheng, S., and Uribe, T., Two-phase densification of cohesive granular aggregates, *Phys. Rev. Lett.*, vol. **88**, no. 20, 204302, 2002.
- Gonzalez, M. and Cuitiño, A. M., A nonlocal contact formulation for confined granular systems, *J. Mech. Phys. Solids*, vol. **60**, no. 2, pp. 333–350, 2012.
- Gonzalez, M. and Cuitiño, A. M., Microstructure evolution of compressible granular systems under large deformations, *J. Mech. Phys. Solids*, in press, 2016.
- Jaeger, H. M., Nagel, S. R., and Behringer, R. P., Granular solids, liquids, and gases, *Rev. Mod. Phys.*, vol. **68**, no. 4, pp. 1259–1273, 1996.
- Johnson, K. L., *Contact Mech.*, Cambridge: Cambridge University Press, 1987.
- Kaganer, M., Contact heat transfer in granular material under vacuum, *J. Eng. Phys.*, vol. **11**, no. 1, pp. 19–22, 1966.
- Küçük, G., Gonzalez, M., and Cuitiño, A. M., Thermo-mechanical behavior of confined granular systems, *Lecture Notes in Applied and Computational Mechanics: Innovative Numerical Approaches for Multi-Field and Multi-Scale Problems*, Springer, 2016.
- Liu, C.-H. and Nagel, S. R., Sound in sand, *Phys. Rev. Lett.*, vol. **68**, no. 15, 2301, 1992.
- Liu, C., Nagel, S. R., Schecter, D., Coppersmith, S., Majumdar, S., Narayan, O., and Witten, T., Force fluctuations in bead packs, *Science*, pp. 513–515, 1995.
- Løvoll, G., Måløy, K. J., and Flekkøy, E. G., Force measurements on static granular materials, *Phys. Rev. E*, vol. **60**, no. 5, 5872, 1999.
- Lu, Z., Abdou, M., and Ying, A., 3d micromechanical modeling of packed beds, *J. Nuclear Mater.*, vol. **299**, no. 2, pp. 101–110, 2001.
- Majmudar, T. S. and Behringer, R. P., Contact force measurements and stress-induced anisotropy in granular materials, *Nature*, vol. **435**, no. 7045, pp. 1079–1082, 2005.
- Makse, H. A., Johnson, D. L., and Schwartz, L. M., Packing of compressible granular materials, *Phys. Rev. Lett.*, vol. **84**, no. 18, pp. 4160–4163, 2000.
- Mueth, D. M., Jaeger, H. M., and Nagel, S. R., Force distribution in a granular medium, *Phys. Rev. E*, vol. **57**, no. 3, 3164, 1998.
- Ostojic, S., Somfai, E., and Nienhuis, B., Scale invariance and universality of force networks in static granular matter, *Nature*, vol. **439**, no. 7078, pp. 828–830, 2006.
- Radjai, F., Jean, M., Moreau, J.-J., and Roux, S., Force distributions in dense two-dimensional granular systems, *Phys. Rev. Lett.*, vol. **77**, no. 2, p. 274, 1996.
- Radjai, F. and Roux, S., Friction-induced self-organization of a one-dimensional array of particles, *Phys. Rev. E*, vol. **51**, no. 6, 6177, 1995.
- Roessig, K. M., Foster, J. C., Jr., and Bardenhagen, S. G., Dynamic stress chain formation in a two-dimensional particle bed, *Exp. Mech.*, vol. **42**, no. 3, pp. 329–337, 2002.
- Rothenburg, L. and Bathurst, R., Analytical study of induced anisotropy in idealized granular materials, *Geotechnique*, vol. **39**, no. 4, pp. 601–614, 1989.
- Siu, W. and Lee, S.-K., Transient temperature computation of spheres in three-dimensional random packings, *Int. J. Heat Mass Transfer*, vol. **47**, no. 5, pp. 887–898, 2004.
- Snoeijer, J. H., Vlugt, T. J., van Hecke, M., and van Saarloos, W., Force network ensemble: A new approach to static granular matter, *Phys. Rev. Lett.*, vol. **92**, no. 5, 054302, 2004.
- Vargas, W. L. and McCarthy, J., Heat conduction in granular materials, *AIChE J.*, vol. **47**, no. 5, pp. 1052–1059, 2001.
- Vargas, W. L. and McCarthy, J., Thermal expansion effects and heat conduction in granular materials, *Phys. Rev. E*, vol. **76**, no. 4, 041301, 2007.
- Zhu, H., Zhou, Z., Yang, R., and Yu, A., Discrete particle simulation of particulate systems: Theoretical developments, *Chem. Eng. Sci.*, vol. **62**, no. 13, pp. 3378–3396, 2007.